



**CD8+ effector memory T cells Marker HLA-B Is a Risk Factor for Atherosclerosis and Prostate Cancer: An Insight Integrating Single-Cell Expression Quantitative Trait Locus and Mendelian Randomization Analyses**

Journal:	Science Progress
Manuscript ID	SCI-25-1475
Manuscript Type:	Original Research Article
Date Submitted by the Author:	02-Jul-2025
Complete List of Authors:	Zhang, Quan; Zunyi Medical University, pan, bochen; Zunyi Medical University
Keywords:	CD8+ Effector Memory T Cells, HLA-B, Atherosclerosis, Prostate Cancer, Single-Cell RNA Sequencing
Abstract:	<p>Abstract</p> <p>Background: atherosclerosis (AS) and Prostate cancer (PCa), though traditionally classified as distinct diseases, share inflammatory and immune dysregulation features, supporting the emerging concept of pan-vascular diseases. This study investigates common immune mechanisms and potential targets across these conditions.</p> <p>Methods: We integrated single-cell RNA sequencing and Mendelian randomization (MR) to profile T cell subsets in PCa, AS, and healthy controls. eQTL mapping and bidirectional MR were conducted to identify causal genes, followed by cell-cell communication and trajectory analyses.</p> <p>Results: CD8+ effector memory T cells (CD8_EM) were enriched in both PCa and AS, displaying shared immune activation patterns. HLA-B, a key CD8_EM marker, was causally linked to PCa and highly expressed in AS. HLA-B+ CD8_EM cells showed stronger signaling and communication activities in diseased tissues.</p> <p>Conclusion: HLA-B may serve as a shared immunological driver in PCa and AS, highlighting its role in the broader context of pan-vascular pathology. These findings offer new insights into shared disease mechanisms and immunotherapeutic strategies for vascular-related malignancies.</p>

**CD8+ effector memory T cells Marker HLA-B Is a Risk Factor for Atherosclerosis and Prostate Cancer: An Insight Integrating Single-Cell Expression Quantitative Trait Locus and Mendelian Randomization Analyses**

Zhangquan<sup>1</sup>, Bochen Pan<sup>1\*</sup>

<sup>1</sup>Key Laboratory of Brain Science, Key Laboratory of Anesthesia and Organ Protection of Ministry of Education (In Cultivation), Zunyi Medical University, Zunyi 563000, Guizhou, China

\*Correspondence: [panbochen0428@163.com](mailto:panbochen0428@163.com)

## Abstract

**Background:** atherosclerosis (AS) and Prostate cancer (PCa), though traditionally classified as distinct diseases, share inflammatory and immune dysregulation features, supporting the emerging concept of pan-vascular diseases. This study investigates common immune mechanisms and potential targets across these conditions.

**Methods:** We integrated single-cell RNA sequencing and Mendelian randomization (MR) to profile T cell subsets in PCa, AS, and healthy controls. eQTL mapping and bidirectional MR were conducted to identify causal genes, followed by cell-cell communication and trajectory analyses.

**Results:** CD8<sup>+</sup> effector memory T cells (CD8\_EM) were enriched in both PCa and AS, displaying shared immune activation patterns. HLA-B, a key CD8\_EM marker, was causally linked to PCa and highly expressed in AS. HLA-B<sup>+</sup> CD8\_EM cells showed stronger signaling and communication activities in diseased tissues.

**Conclusion:** HLA-B may serve as a shared immunological driver in PCa and AS, highlighting its role in the broader context of pan-vascular pathology. These findings offer new insights into shared disease mechanisms and immunotherapeutic strategies for vascular-related malignancies.

**Keywords:** CD8<sup>+</sup> Effector Memory T Cells, HLA-B, Atherosclerosis, Prostate Cancer, Single-Cell RNA Sequencing

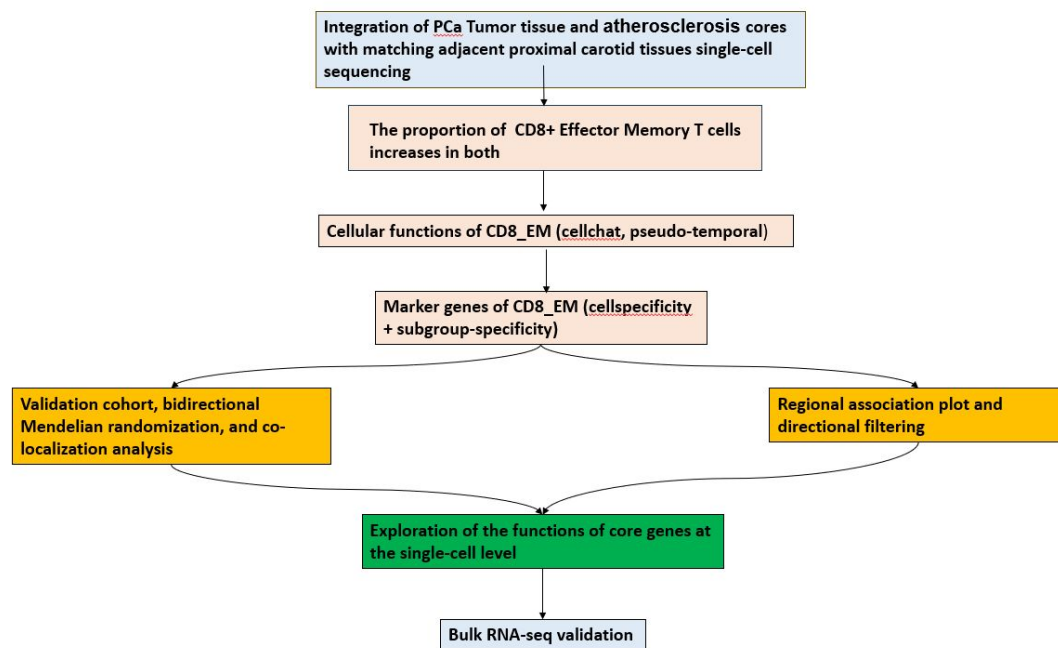
**Introduction**

Prostate cancer (PCa) is the most prevalent urogenital tumor in men globally, affecting over 1.4 million individuals and causing more than 375,000 deaths annually[1]. As one of the most common male malignancies, it primarily targets the prostate gland. The cancer often progresses slowly and initially relies on androgens, but it can evolve into castration-resistant prostate cancer (CRPC), resistant to standard androgen deprivation therapy [2, 3]. Early detection includes PSA testing, rectal exams, and imaging [4]. Treatment options encompass surgery, radiotherapy, hormone therapy, chemotherapy, and increasingly, immunotherapy and targeted therapies for advanced cases [5].

Atherosclerosis (AS) is a systemic vascular disorder characterized by arterial wall inflammation and plaque formation, representing a major component of panvascular diseases[6, 7]. It is a leading cause of heart disease, stroke, and peripheral artery disease, underscoring its role in global morbidity and mortality. The condition begins with endothelial cell activation, which triggers vessel narrowing and inflammation, leading to plaque formation. Notably, AS shares pathophysiological similarities with cancer, including chronic inflammation, metabolic reprogramming, and immune dysregulation[8, 9]. For instance, recent studies highlight the oncogenic-like behavior of vascular smooth muscle cells (SMCs), such as their ability to undergo proliferation, resist apoptosis, and remodel the extracellular matrix—phenomena also observed in tumor cells[10, 11]. These parallels have led to the emergence of "pan-cardio-oncology", a paradigm that seeks to unravel shared molecular mechanisms between vascular diseases and cancer[12, 13].

Inflammation may bridge lipid abnormalities and AS progression [8, 9]. Studies suggest that high-sensitivity C-reactive protein (hsCRP) independently predicts cardiovascular events [10, 11]. In rodent models, mutations in genes linked to clonal hematopoiesis, such as Dnmt3a, Tet2, or Jak2 V617F, accelerate AS and activate pro-inflammatory pathways [12, 13]. These insights advance understanding and treatment of AS, though further research is needed to fully uncover its mechanisms and risk mitigation strategies. Importantly, clonal hematopoiesis-associated mutations have also been implicated in the development of certain cancers, including PCa, underscoring the genetic and immunological overlap between AS and malignancies [13].

This study aims to identify potential therapeutic targets shared between AS and PCa through Mendelian randomization (MR) analysis, integrating eQTL data from blood samples with two independent PCa Genome-Wide Association Study (GWAS) datasets. We specifically focus on the association between the HLA-B gene and PCa. The findings from this study could provide new insights into the shared molecular mechanisms underlying these diseases and highlight potential therapeutic targets for both AS and PCa. The workflow for this study is outlined in Figure 1.



## Methods

### Data collection

We downloaded STAR count data and clinical information for 52 normal samples and 499 PCa samples from the UCSC Xena website (<https://xena.ucsc.edu/>). TPM format data was extracted and normalized using  $\log_2(\text{TPM} + 1)$ . We retained samples with RNAseq data and clinical information for further analysis.

Additionally, the datasets (GSE100927, GSE159677, GSE216860, and GSE141445) were retrieved from the GEO database (<https://www.ncbi.nlm.nih.gov/>). We conducted transcriptomic analysis of human peripheral arteries in the carotid, femoral, and popliteal regions from atherosclerotic and control tissues. Furthermore tumor cells from 13 PCa patients (GSM4203181), normal tissues from 6 healthy individuals

(GSM6696842,GSM6696843,GSM6696844,GSM6696845,GSM6696846,GSM6696847), and atherosclerotic cores with matching adjacent proximal carotid tissues from 3 AS patients (GSM4837523, GSM4837524, GSM4837525, GSM4837526, GSM4837527,GSM4837528) were selected for 10X single-cell sequencing. The SNPs used as genetic instruments were sourced from a comprehensive European GWAS (<https://gwas.mrcieu.ac.uk/>)[14-16].

**Single-cell data processing and analysis**

Single-cell RNA-seq data from normal, atherosclerotic, and tumor tissues were processed using the Seurat pipeline. Individual Seurat objects were created for each sample and merged into a unified object for integrated analysis. Cells with high mitochondrial or red blood cell gene expression were excluded during quality control. Following normalization, principal component analysis (PCA) was conducted on the top 2,000 highly variable genes. Batch effects were corrected using the Harmony algorithm, and clustering was performed using UMAP for dimensionality reduction. Cell-type annotation was based on canonical markers from the CellMarker database, visualized via FeaturePlot and DimPlot. After manual verification, differential expression analysis was performed using a fold change threshold of 1.5 and an adjusted p-value < 0.05, with results visualized through volcano plots and heatmaps. For developmental trajectory reconstruction, Monocle was employed, while CellChat was used to model intercellular communication.

**CD8\_EM key marker gene eQTL and PCa's mendelian randomization analysis**

CD8\_EM marker genes were identified through comparison with other T cell subsets. Gene symbols were converted to ENSEMBL IDs, and SNPs associated with these markers were extracted from the "ieu-b-4809" GWAS dataset. SNPs passing an eQTL p-value threshold of  $5 \times 10^{-8}$  were retained.  $R^2$  and F-statistics were calculated to assess instrument strength. TwoSampleMR was used to estimate causal associations between candidate genes and PCa.

**Validation set MR analysis, bidirectional Mendelian MR and colocalization analysis**

Validation analysis was conducted by harmonizing exposure and outcome datasets, followed by causal inference using the mr\_modified function, which also calculated the phenotypic

variance explained (PVE). Forest plots were generated for visualization. For bidirectional MR, SNPs from the reverse exposure dataset ("ebi-a-GCST90018905") were merged with outcome data to generate a harmonized PCa gene set. eQTL data were processed using `vcfR`, and `coloc.abf` was applied to assess colocalization using Bayes factor estimation. The results were interpreted according to standard colocalization hypotheses and evidence strength.

### **Regional association plot**

Construct a regional association plot. By reading the genotype data from `eql-a-ENSG00000234745.vcf` (in VCF format) and the related association data, extract the eQTL information associated with the target gene. Based on this, select the eQTLs located within the specified region and organize them into a format suitable for plotting a regional association plot. The plotting process uses the `locuscomparer` package to visualize the association information from both eQTL and GWAS, providing an intuitive graphical presentation for subsequent analysis.

### **Single-cell Functional Analysis of Exposure-Associated Genes**

To investigate the functional role of target genes at the single-cell level, we visualized their expression patterns using `DotPlot` and `FeaturePlot` in `Seurat`. Developmental trajectories were reconstructed with the `Slingshot` package, with dimensionality reduction performed via `UMAP`. Key trajectory-driving genes were identified using the `find_switch_logistic_fastglm` function, and gene expression dynamics were illustrated along pseudotime using `plot_timeline_ggplot`. Intercellular communication analysis was conducted with the `CellChat` tool. This included identifying ligand–receptor pairs, mapping interactions to protein–protein interaction networks, and calculating communication probabilities. The network structure was visualized using `netVisual_circle` and `netVisual_bubble`. Additionally, differential gene expression analysis was performed by integrating bulk transcriptomic datasets to validate single-cell findings and assess consistency across platforms.

### **Trajectory inference**

We used the `monocle3` package in R [17, 18] to infer T cell differentiation trajectories.

1  
2  
3  
4  
5  
6  
7  
8  
9  
10  
11  
12  
13  
14  
15  
16  
17  
18  
19  
20  
21  
22  
23  
24  
25  
26  
27  
28  
29  
30  
31  
32  
33  
34  
35  
36  
37  
38  
39  
40  
41  
42  
43  
44  
45  
46  
47  
48  
49  
50  
51  
52  
53  
54  
55  
56  
57  
58  
59  
60

The process began with data preprocessing, including quality control, normalization, and dimensionality reduction. Parameters were then configured following the guidelines in the official documentation, leading to cell state inference and transcriptome trajectory analysis.

**Data analysis**

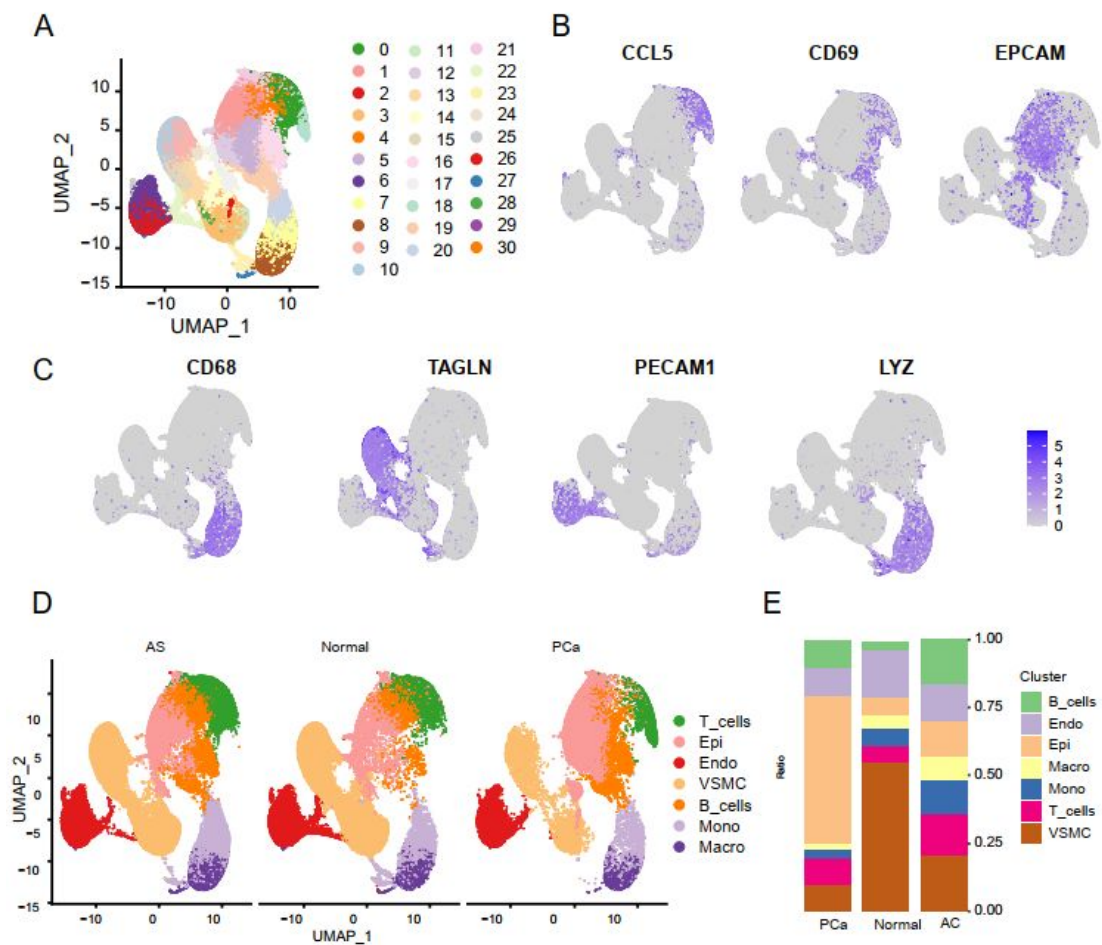
All data analyses were performed based on R 4.2.1, with  $p < 0.05$  considered statistically significant.

For Peer Review

## Results

### Single-cell transcriptomic analysis of PCa, AS and normal groups

In this study, we selected 13 PCa samples, 6 healthy controls, and 3 groups of AS samples from the datasets GSE159677, GSE216860, and GSE141445 for 10X single-cell RNA sequencing analysis. Low-quality data was initially filtered out (Fig.S1 A-B), leaving 64,568 cells for further analysis. To reduce batch effects across samples, we used the Harmony method for integration and standardization, followed by normalization, PCA for dimensionality reduction, and clustering (Fig.S1 C). Visualization of each cluster was achieved using UMAP based on the top 15 principal components (Fig.S1 D). Specific marker genes were then used to identify and annotate different cell subpopulations in the single-cell RNA sequencing data. We annotated the clusters using the RenameIdents function, aligning each with its corresponding cell type. Cell distribution was visualized with UMAP and DimPlot (Fig.2 A). FeaturePlot in Seurat was used to display the spatial distribution of marker genes for various cell types, including T cells, epithelial cells, endothelial cells, vascular smooth muscle cells, B cells, macrophages, and monocytes. (Fig.2 B, C). Manual annotation renamed 30 clusters, visualized by UMAP and DimPlot, segmented by tissue type (Fig.2 D). Figure 2E shows significant differences in T and epithelial cell proportions across samples, highlighting the importance of understanding T cell functions in cancer and AS for effective treatments.

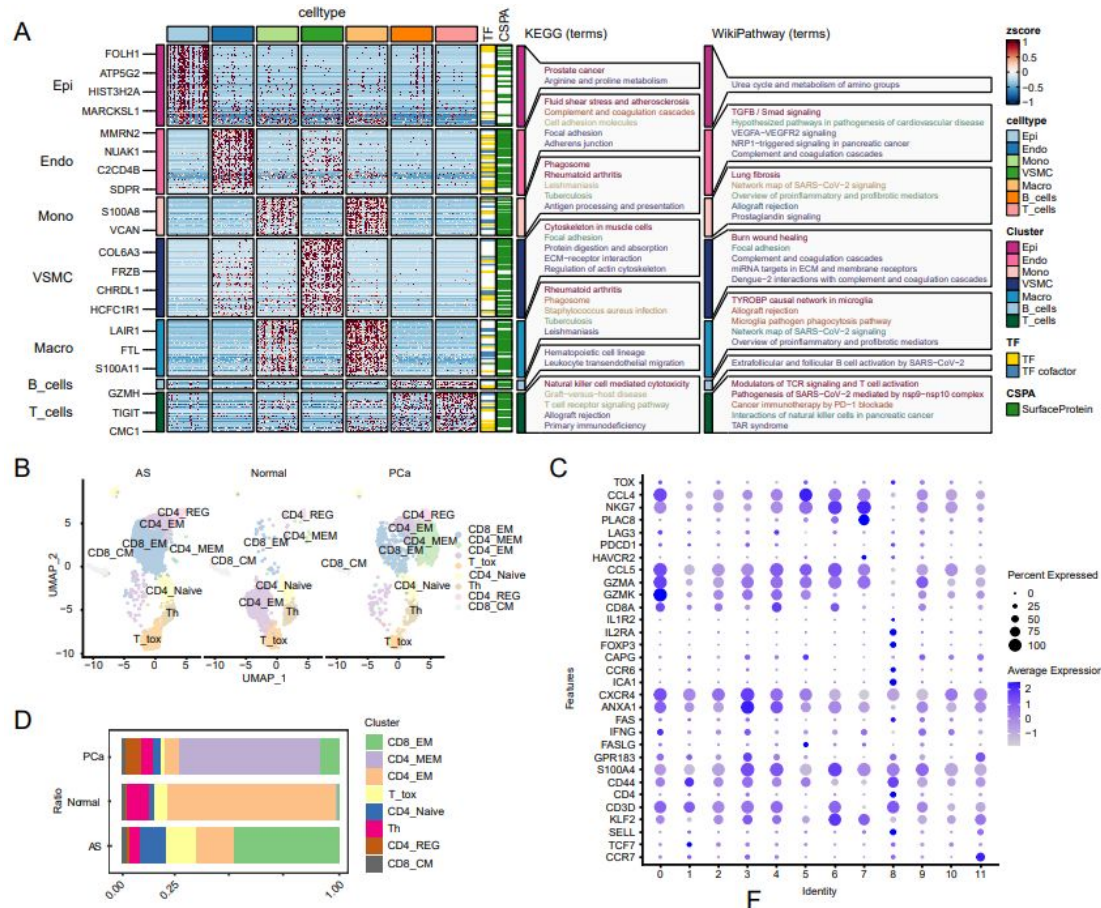


### KEGG and WikiPathway enrichment analysis and single-cell transcriptomics of T cells

We performed differential gene expression analysis across seven cell types—T cells, epithelial cells, endothelial cells, vascular smooth muscle cells, B cells, monocytes, and macrophages—defining genes with fold change  $\geq 1.5$  or  $\leq -1.5$  as differentially expressed. To explore functional roles of differentially expressed T cell genes, we conducted enrichment analyses using TF, CSPA, GO\_BP, KEGG, and WikiPathway databases (Fig. 2A). KEGG analysis revealed enrichment in NK cell-mediated cytotoxicity, while WikiPathway indicated involvement in NK cell interactions in PCa, TCR signaling, and T cell activation. These findings highlight the distinct biological roles of T cells in immune responses and disease.

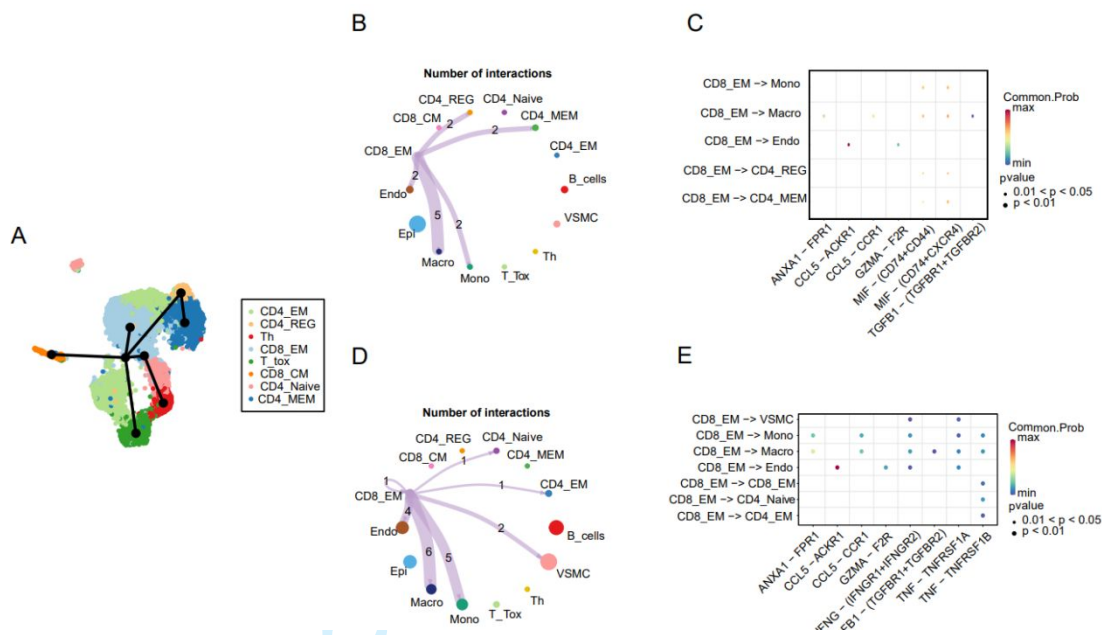
We then isolated T cell subpopulations from the single-cell RNA-seq data, followed by standard preprocessing, dimensionality reduction, clustering, and manual annotation. Eight T cell clusters were identified and visualized by tissue type (Fig. 3B). A dot plot illustrated marker

gene expression across subpopulations (Fig. 3C), and a cell proportion plot showed a significant increase in CD8\_EM cells in cancer and AS groups versus normal (Fig. 3D). These results offer valuable insights for downstream analysis.



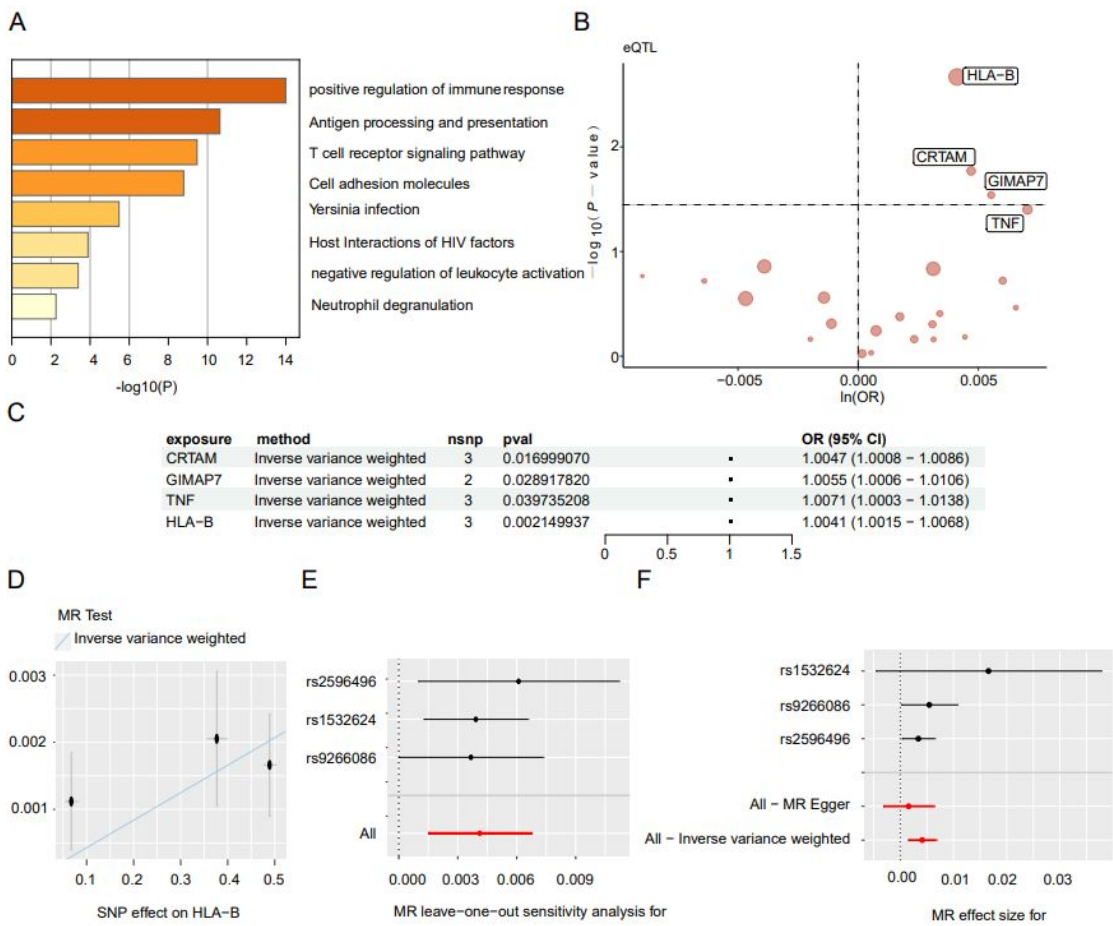
## Trajectory analysis of T cell types and cell communication

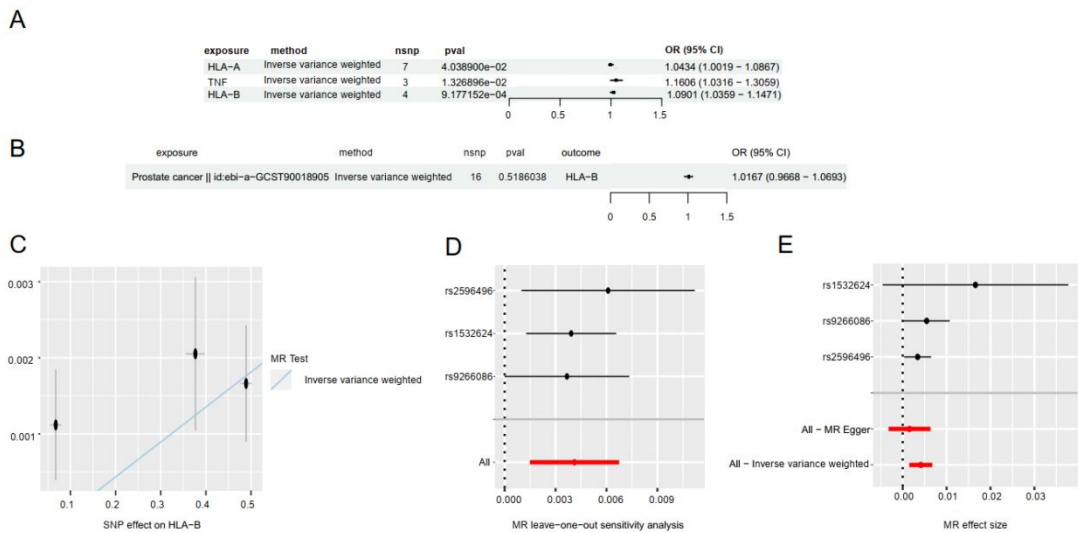
Using single-cell RNA sequencing and the Slingshot R package, we reconstructed T cell differentiation trajectories. UMAP visualization effectively captured the continuous nature of T cell development, identifying CD4\_Naïve as the root and CD8\_EM as a differentiated branch, suggesting that CD8\_EM cells arise from CD8<sup>+</sup> T cells after antigen stimulation (Fig. 4A). To further explore the functional role of CD8\_EM cells in PCa and AS, we performed cell-cell communication analysis. In both diseases, CD8\_EM cells exhibited frequent interactions with endothelial cells, primarily via the CCL5-ACKR1 signaling pathway (Fig. 4B-E). These findings underscore the significance of CD8\_EM cells as central mediators of immune communication in the disease microenvironment.



MR analysis using key marker genes identifies one novel causal gene for PCa

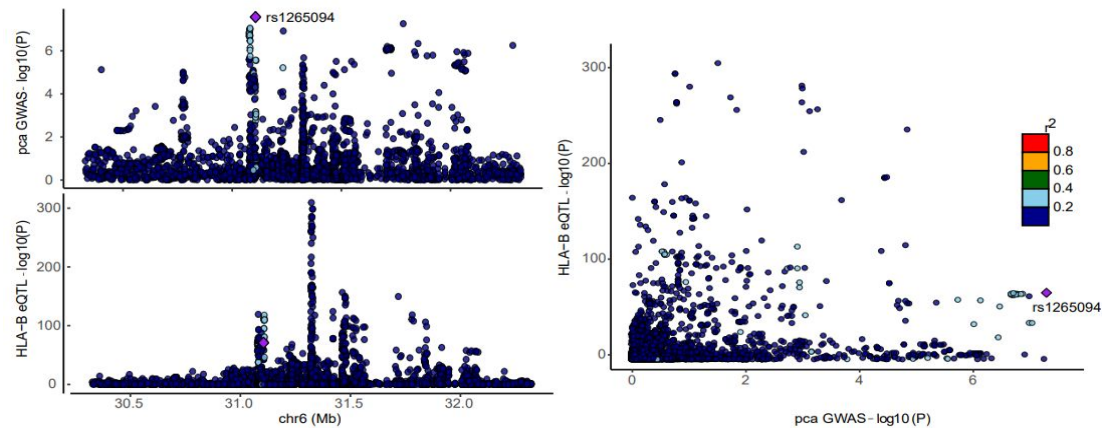
We identified 30 key genes specifically expressed in CD8\_EM cells using Seurat (Table S1). These genes distinguish CD8\_EM T cells from other subtypes and serve as crucial markers for downstream analyses. Enrichment analysis via Metscape linked them to pathways such as "positive regulation of programmed cell death," "antigen processing and presentation," and "T cell receptor signaling" (Fig. 5A). To assess potential associations with prostate cancer (PCa), we performed two-sample Mendelian randomization (MR) using scRNA-seq data. Gene symbols were converted to ENSEMBL IDs via org.Hs.eg.db. SNPs related to target genes were extracted as exposures, and PCa outcome data were obtained from the EBI database. Integration of these datasets revealed several genes significantly associated with PCa risk: CRTAM (OR=1.0047, p=0.0169), GIMAP7 (OR=1.0055, p=0.0289), TNF (OR=1.0071, p=0.039), and HLA-B (OR=1.0041, p=0.0021). A volcano plot (-log10 p vs ln(OR), Fig. 5B) and forest plots (Fig. 5C–F) visualize these associations. No significant heterogeneity or horizontal pleiotropy was observed for CRTAM, TNF, and HLA-B (Table S2–S3), supporting the robustness of our findings. These results point to potential genetic markers for PCa risk and offer directions for future biological validation.





### Investigating the association between the HLA-B gene and PCa using Mendelian Randomization

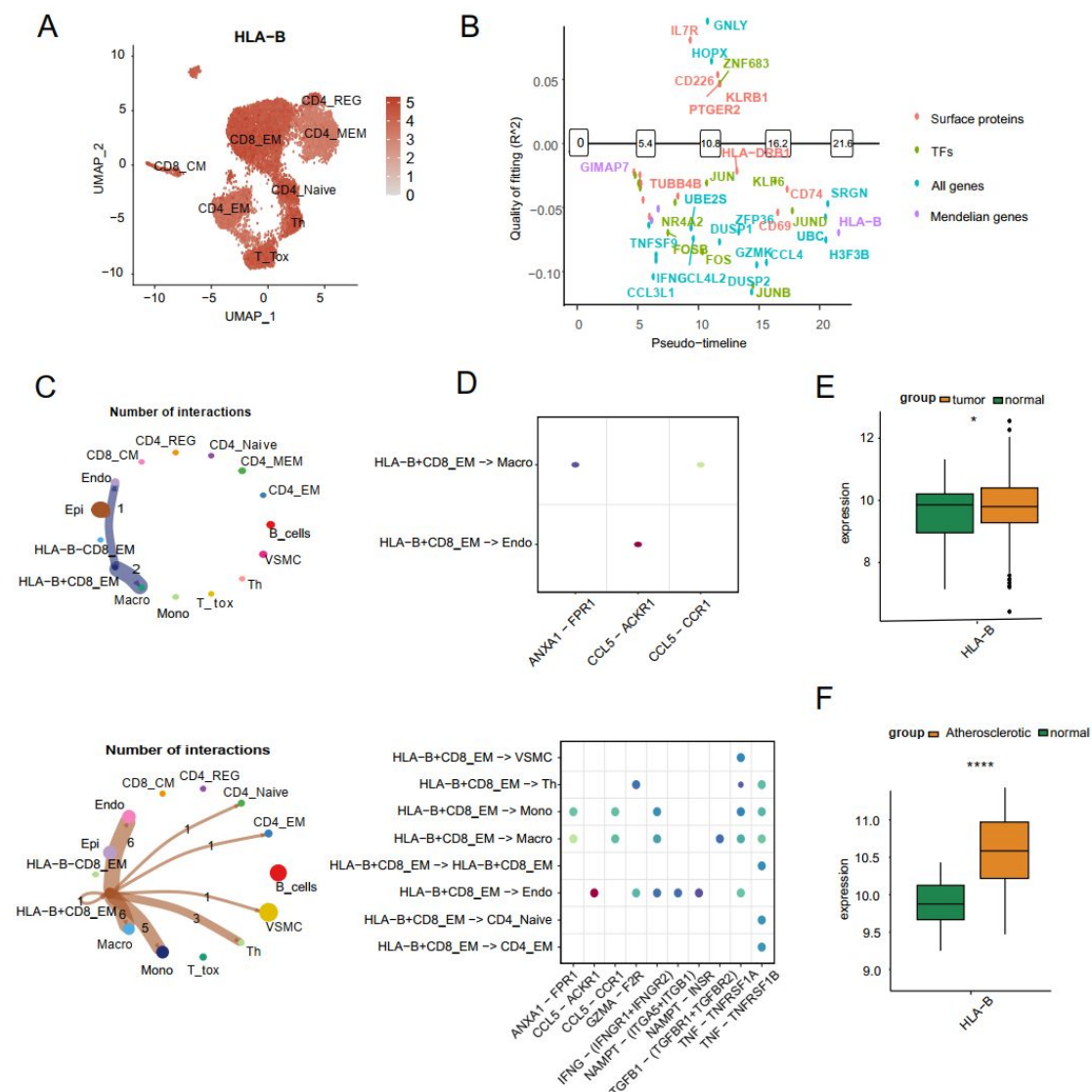
In this study, we presented the eQTL regional association plot for the HLA-B gene and the PCa GWAS results. By comparing the association strengths, we identified several SNPs that showed strong associations with both phenotypes. Notably, certain SNPs related to HLA-B eQTLs (eg: rs1265094) also exhibited significant associations in the PCa GWAS. This provides preliminary evidence for a potential link between the HLA-B gene and PCa development (Figure 6).



### Single-cell transcriptome analysis reveals the critical role of HLA-B in T cell function within PCa and AS

We analyzed the expression dynamics of HLA-B across cell populations and pseudotime. FeaturePlot revealed that HLA-B is highly expressed in specific cell clusters (Fig. 8A), with increased expression during early-to-mid stages of T cell development and a decline in later

stages (Fig. 8B). In both PCa and AS groups, CellChat analysis showed that HLA-B<sup>+</sup> CD8<sub>EM</sub> cells exhibited stronger intercellular communication and more active ligand-receptor interactions than their HLA-B<sup>-</sup> counterparts (Fig. 8C). Notably, the CCL5–ACKR1 signaling pathway was prominently enriched in HLA-B<sup>+</sup> CD8<sub>EM</sub>-mediated interactions (Fig. 8D). Differential expression analysis confirmed that HLA-B<sup>+</sup> CD8<sub>EM</sub> cells are linked to PCa-associated genes. Furthermore, HLA-B expression levels were significantly higher in PCa and AS samples compared to healthy controls (Fig. 8E–F), reinforcing its potential role as a functional immune modulator in disease states.



**Discussion**

PCa, one of the most common male malignancies, initially relies on androgens but can progress to CRPC. It is often described as an "immune-cold" tumor, characterized by fewer gene mutations in tumor cells, reduced antigen presentation, and lower CD8+ T cell activation, alongside higher levels of immunosuppressive molecules like cytokines and chemokines [19, 20]. CD8+ T cells recognize antigen peptides presented by MHC class I molecules and eliminate target cells through perforin and granzyme release, making their function crucial in anti-tumor immunity and increasingly vital in cancer immunotherapy [21, 22]. CD8+ T cells include two circulating memory subpopulations: CD8\_EM and CD8\_CM. CD8\_EM, or effector memory CD8+ T cells, are a subset within the CD8+ T cell lineage that can rapidly respond to tumor recurrence, playing a crucial role in the adaptive immune system[23, 24]. They are primarily found in peripheral blood, peripheral tissues, and secondary lymphoid organs[25]. Although CD8\_CM cells have stronger antitumor effects, CD8\_EM cells are more widely distributed throughout the body, particularly in non-lymphoid tissues, enabling a faster response to infections or tumors [26].

The CD8+ T cells induced by this vaccine are crucial for protective immune responses and play a key role in PCa treatment, particularly through their involvement in immune surveillance and antitumor activity. However, in PCa patients, CD8\_EM cells may become dysfunctional and inactive due to prolonged antigen exposure in chronic infections or the tumor microenvironment (TME) [27-30]. Within the TME, immune suppression occurs through (1) differential mutations that regulate immune responses [31-33] and (2) tumor-infiltrating T cells that induce checkpoint molecules and recruit immunosuppressive cells [34-36]. In PCa tissue, the number of CD8\_EM cells is lower compared to peripheral blood, with reduced cytokine secretion capacity. Many PCa patients exhibit immune ignorance, partly due to the tumor microenvironment (TME) suppressing CD8\_EM cell activity through mechanisms like the CTLA4, PD-1, PD-L1/2, and TGF- $\beta$  pathways. CTLA-4 and PD-1 are immune checkpoint molecules that inhibit T cell activation[37], while PD-L1/2 binds to PD-1, further suppressing T cell function[38]. TGF- $\beta$  enhances this suppression by promoting an immunosuppressive environment[39]. Enhancing CD8\_EM cell infiltration and activity through immunotherapy is

a key approach to boosting antitumor immunity in PCa patients. Studies have shown that using anti-CTLA-4, anti-PD-1, or anti-PD-L1 antibodies, as well as TGF- $\beta$  inhibitors, can partially restore the activity and function of CD8<sub>EM</sub> cells within tumors [40-43]. The subpopulation and functional state of CD8<sub>EM</sub> cells can serve as important biomarkers for predicting and monitoring the effectiveness of PCa immunotherapy. In summary, the subpopulation and functional state of CD8<sub>EM</sub> cells are crucial for immune responses in tumor immunity. Further exploration of their biology and function, coupled with immunotherapeutic strategies, could advance antitumor treatments.

This study systematically examined the composition and function of immune cells in AS and PCa patients as well as healthy individuals using scRNA-seq analysis. Our preliminary data confirmed the presence of T cells, B cells, epithelial cells, and others in the tumor tissue of PCa patients and the atherosclerotic core and matching carotid tissue in AS patients, consistent with existing literature[44-46]. Notably, both AS and PCa patient groups showed an increased proportion of effector memory CD8<sup>+</sup> T cells (CD8<sub>EM</sub>) compared to healthy controls, potentially linked to disease characteristics.

Additionally, single-cell trajectory analysis has revealed the dynamic differentiation process of T cells, offering new insights into T cell development and activation. The analysis of cell communication networks also showed enhanced interactions between CD8<sub>EM</sub> T cells and endothelial cells, suggesting their role in regulating other immune cells during disease progression. This study not only identifies disease-related immune cell changes but also proposes potential molecular mechanisms through multi-omics analysis. For example, we found that increased HLA-B expression might contribute to the reduced function of CD8<sup>+</sup> T cells. HLA-B is a T cell receptor gene involved in antigen recognition and is part of the major histocompatibility complex I (MHC-I) [47]. While high HLA-B expression can enhance the immune system's ability to recognize and kill tumor cells, its high polymorphism means different HLA-B alleles are linked to PCa susceptibility [48-51]. In the tumor microenvironment, excessive HLA-B expression may cause immune cells, including T and B lymphocytes, and NK cells, to lose their function [52]. Therefore, regulating HLA-B expression levels could be a new strategy to enhance T cell antitumor activity.

It is important to acknowledge certain limitations in this study. First, due to the limited

sample size, the results require validation in larger cohorts. Additionally, the predicted functional roles of key genes need further experimental validation, and molecular mechanisms should be explored using animal models. Furthermore, the inherent batch effects of scRNA-seq technology may affect the interpretation of results, so future research should increase sample size and use standardized procedures for verification. Lastly, MR analysis may produce false positives due to genetic pleiotropy, necessitating functional validation of new candidate genes.

**Conclusion**

This study provides a comprehensive integrative analysis combining single-cell transcriptomics and Mendelian randomization to uncover shared immune mechanisms underlying AS and PCa. We identified (CD8\_EM as a common immunological feature in both diseases, characterized by increased proportions and enhanced cell-cell communication. Among CD8\_EM-associated genes, HLA-B emerged as a robust genetic risk factor for PCa and was also highly expressed in AS tissues. Functional analyses revealed that HLA-B<sup>+</sup> CD8\_EM cells exhibit stronger intercellular signaling and play a central role in immune modulation within diseased microenvironments. Bidirectional and validation MR analyses supported the causal role of HLA-B in PCa risk, while single-cell trajectory and pseudotime analyses highlighted its involvement in T cell development and dysfunction. These findings suggest that HLA-B may serve as a potential immunological driver and therapeutic target across pan-vascular conditions. Future studies should validate these observations in larger cohorts and explore the therapeutic implications of modulating HLA-B-mediated immune responses.

## Figure legend

**Figure 1.** The workflow of the present study

**Figure 2.** Single-cell transcriptomics overview across various samples. (A). UMAP plot colored by various cell clusters. (B) and (C). UMAP plots showing representative marker genes for each cell type. (D). After manual annotation, seven distinct cell groups were identified: T cells, epithelial cells, endothelial cells, vascular smooth muscle cells, B cells, monocytes, and macrophages. (E). The proportion of each cell type across different samples is displayed as shown in the figure.

**Figure 3:** In-depth analysis and visualization of T cell subpopulations. (A). KEGG and WikiPathway enrichment analysis. (B). Manually annotated T cell subpopulations. (C). Dot plot illustrating the expression of characteristic genes across various cell subpopulations. (D). Distribution of T cell subpopulations across different samples.

**Figure 4:** Cellular Differentiation and Communication Analysis in AS and PCa. (A). UMAP plot showing the cell differentiation trajectory. (B, D). Cell communication networks constructed for CD8\_CM and other cells in PCa and AS samples. (C, E). Differentially enriched signaling pathway analysis between CD8\_EM and other cells in PCa and AS samples.

**Figure 5** Shows the Mendelian Randomization analysis: (A). Bar chart of gene set enrichment analysis. (B). A volcano plot illustrating the association between key genes and PCa risk. (C). A forest plot describing the association between key genes and PCa risk. (D). A scatter plot showing the genetic association between "HLA-B" and PCa. (E). A forest plot of single nucleotide polymorphisms related to "HLA-B" and their causal relationship with PCa. (F). The validity and robustness of the Mendelian Randomization results, further validating the identified associations with minimal bias and confounding factors.

**Figure 6.** Validation cohort and bidirectional Mendelian Randomization (A). Mendelian Randomization analysis shows the association between HLA-B gene variants and PCa risk. (B). Reverse Mendelian Randomization illustrates the relationship between PCa and the HLA-B gene. (C). Scatter plot in the validation cohort displays the genetic association between "HLA-B" and PCa. (D). Forest plot in the validation cohort examines the causal relationship of single nucleotide polymorphisms related to "HLA-B" and PCa. (E). Demonstrates the validity and robustness of Mendelian Randomization in the validation cohort.

**Figure 7.** Regional association map

**Figure 8.** Single-cell transcriptome analysis reveals the critical role of HLA-B in T cell metabolism and function in PCa. (A). UMAP plot showing the distribution of HLA-B gene expression in cells. (B). Gene on/off states in pseudo-time, reflecting gene expression dynamics during cell development or transcriptional processes. (C). Intercellular communication between HLA-B+CD8\_EM and HLA-B-CD8\_EM cell subpopulations in PCa and AS analyzed using the CellChat tool, with the top showing results from the PCa group and the bottom showing results from the AS group. (D). Differential signaling pathway enrichment involving HLA-B+CD8\_EM and HLA-B-CD8\_EM cells compared to other cells, shown in order from top to bottom for the PCa group and the AS group. (E). This boxplot illustrates the expression levels of the HLA-B gene in PCa group and Normal Group (F). This boxplot illustrates the expression levels of the HLA-B gene in AS group and Normal Group.

Reference

1. Ferlay J, Colombet M, Soerjomataram I, Parkin DM, Piñeros M, Znaor A, Bray F: **Cancer statistics for the year 2020: An overview.** *International journal of cancer* 2021.

2. Gamat M, McNeel DG: **Androgen deprivation and immunotherapy for the treatment of prostate cancer.** *Endocrine-related cancer* 2017, **24**(12):T297-t310.

3. Teo MY, Rathkopf DE, Kantoff P: **Treatment of Advanced Prostate Cancer.** *Annual review of medicine* 2019, **70**:479-499.

4. Olkowski C, Fernandes B, Griffiths GL, Lin F, Choyke PL: **Preclinical Imaging of Prostate Cancer.** *Seminars in nuclear medicine* 2023, **53**(5):644-662.

5. Evans AJ: **Treatment effects in prostate cancer.** *Modern pathology : an official journal of the United States and Canadian Academy of Pathology, Inc* 2018, **31**(S1):S110-121.

6. Herrington W, Lacey B, Sherliker P, Armitage J, Lewington S: **Epidemiology of Atherosclerosis and the Potential to Reduce the Global Burden of Atherothrombotic Disease.** *Circulation research* 2016, **118**(4):535-546.

7. Roth GA, Mensah GA, Johnson CO, Addolorato G, Ammirati E, Baddour LM, Barengo NC, Beaton AZ, Benjamin EJ, Benziger CP *et al*: **Global Burden of Cardiovascular Diseases and Risk Factors, 1990-2019: Update From the GBD 2019 Study.** *Journal of the American College of Cardiology* 2020, **76**(25):2982-3021.

8. Kowara M, Cudnoch-Jedrzejewska A: **Pathophysiology of Atherosclerotic Plaque Development-Contemporary Experience and New Directions in Research.** *International journal of molecular sciences* 2021, **22**(7).

9. Simionescu M: **Implications of early structural-functional changes in the endothelium**

- for vascular disease. *Arteriosclerosis, thrombosis, and vascular biology* 2007, **27**(2):266-274.
10. Ridker PM: **A Test in Context: High-Sensitivity C-Reactive Protein.** *Journal of the American College of Cardiology* 2016, **67**(6):712-723.
11. Ridker PM, Koenig W, Kastelein JJ, Mach F, Lüscher TF: **Has the time finally come to measure hsCRP universally in primary and secondary cardiovascular prevention?** *European heart journal* 2018, **39**(46):4109-4111.
12. Fuster JJ, MacLauchlan S, Zuriaga MA, Polackal MN, Ostriker AC, Chakraborty R, Wu CL, Sano S, Muralidharan S, Rius C *et al.*: **Clonal hematopoiesis associated with TET2 deficiency accelerates atherosclerosis development in mice.** *Science (New York, NY)* 2017, **355**(6327):842-847.
13. Jaiswal S, Natarajan P, Silver AJ, Gibson CJ, Bick AG, Shvartz E, McConkey M, Gupta N, Gabriel S, Ardissino D *et al.*: **Clonal Hematopoiesis and Risk of Atherosclerotic Cardiovascular Disease.** *The New England journal of medicine* 2017, **377**(2):111-121.
14. Hicks C, Koganti T, Giri S, Tekere M, Ramani R, Sitthi-Amorn J, Vijayakumar S: **Integrative genomic analysis for the discovery of biomarkers in prostate cancer.** *Biomarker insights* 2014, **9**:39-51.
15. Jiang J, Cui W, Vongsangnak W, Hu G, Shen B: **Post genome-wide association studies functional characterization of prostate cancer risk loci.** *BMC genomics* 2013, **14** Suppl 8(Suppl 8):S9.
16. Mountjoy E, Schmidt EM, Carmona M, Schwartzentruber J, Peat G, Miranda A, Fumis L, Hayhurst J, Buniello A, Karim MA *et al.*: **An open approach to systematically prioritize**

causal variants and genes at all published human GWAS trait-associated loci. *Nature genetics* 2021, **53**(11):1527-1533.

17. Kannan S, Miyamoto M, Zhu R, Lynott M, Guo J, Chen EZ, Colas AR, Lin BL, Kwon C: **Trajectory reconstruction identifies dysregulation of perinatal maturation programs in pluripotent stem cell-derived cardiomyocytes.** *Cell reports* 2023, **42**(4):112330.

18. Tran B, Tran D, Nguyen H, Ro S, Nguyen T: **scCAN: single-cell clustering using autoencoder and network fusion.** *Scientific reports* 2022, **12**(1):10267.

19. Bou-Dargham MJ, Sha L, Sang QA, Zhang J: **Immune landscape of human prostate cancer: immune evasion mechanisms and biomarkers for personalized immunotherapy.** *BMC cancer* 2020, **20**(1):572.

20. Wang L, Geng H, Liu Y, Liu L, Chen Y, Wu F, Liu Z, Ling S, Wang Y, Zhou L: **Hot and cold tumors: Immunological features and the therapeutic strategies.** *MedComm* 2023, **4**(5):e343.

21. Chen Y, Yu D, Qian H, Shi Y, Tao Z: **CD8(+) T cell-based cancer immunotherapy.** *Journal of translational medicine* 2024, **22**(1):394.

22. Kumar S, Singh SK, Rana B, Rana A: **Tumor-infiltrating CD8(+) T cell antitumor efficacy and exhaustion: molecular insights.** *Drug discovery today* 2021, **26**(4):951-967.

23. Lanzavecchia A, Sallusto F: **Understanding the generation and function of memory T cell subsets.** *Current opinion in immunology* 2005, **17**(3):326-332.

24. Sallusto F, Geginat J, Lanzavecchia A: **Central memory and effector memory T cell subsets: function, generation, and maintenance.** *Annual review of immunology* 2004, **22**:745-763.

- 1  
2  
3  
4 25. Jung YW, Rutishauser RL, Joshi NS, Haberman AM, Kaech SM: **Differential**  
5  
6 **localization of effector and memory CD8 T cell subsets in lymphoid organs during acute**  
7  
8 **viral infection.** *Journal of immunology (Baltimore, Md : 1950)* 2010, **185**(9):5315-5325.  
9  
10  
11 26. Han J, Khatwani N, Searles TG, Turk MJ, Angeles CV: **Memory CD8(+) T cell**  
12  
13 **responses to cancer.** *Seminars in immunology* 2020, **49**:101435.  
14  
15  
16 27. Kim SK, Cho SW: **The Evasion Mechanisms of Cancer Immunity and Drug Intervention**  
17  
18 **in the Tumor Microenvironment.** *Frontiers in pharmacology* 2022, **13**:868695.  
19  
20  
21 28. Kwon OJ, Zhang L, Ittmann MM, Xin L: **Prostatic inflammation enhances basal-to-**  
22  
23 **luminal differentiation and accelerates initiation of prostate cancer with a basal cell**  
24  
25 **origin.** *Proceedings of the National Academy of Sciences of the United States of*  
26  
27 *America* 2014, **111**(5):E592-600.  
28  
29  
30 29. Mani RS, Amin MA, Li X, Kalyana-Sundaram S, Veeneman BA, Wang L, Ghosh A,  
31  
32 Aslam A, Ramanand SG, Rabquer BJ *et al*: **Inflammation-Induced Oxidative Stress**  
33  
34 **Mediates Gene Fusion Formation in Prostate Cancer.** *Cell reports* 2016, **17**(10):2620-  
35  
36 2631.  
37  
38  
39 30. Sfanos KS, Yegnasubramanian S, Nelson WG, De Marzo AM: **The inflammatory**  
40  
41 **microenvironment and microbiome in prostate cancer development.** *Nature reviews*  
42  
43 *Urology* 2018, **15**(1):11-24.  
44  
45  
46 31. Agupitan AD, Neeson P, Williams S, Howitt J, Haupt S, Haupt Y: **P53: A Guardian of**  
47  
48 **Immunity Becomes Its Saboteur through Mutation.** *International journal of molecular*  
49  
50 *sciences* 2020, **21**(10).  
51  
52  
53 32. Guo G, Yu M, Xiao W, Celis E, Cui Y: **Local Activation of p53 in the Tumor**  
54  
55  
56  
57  
58  
59  
60

- Microenvironment Overcomes Immune Suppression and Enhances Antitumor Immunity. *Cancer research* 2017, **77**(9):2292-2305.
33. Kogan D, Grabner A, Yanucil C, Faul C, Ulaganathan VK: **STAT3-enhancing germline mutations contribute to tumor-extrinsic immune evasion.** *The Journal of clinical investigation* 2018, **128**(5):1867-1872.
34. Jarnicki AG, Lysaght J, Todryk S, Mills KH: **Suppression of antitumor immunity by IL-10 and TGF-beta-producing T cells infiltrating the growing tumor: influence of tumor environment on the induction of CD4+ and CD8+ regulatory T cells.** *Journal of immunology (Baltimore, Md : 1950)* 2006, **177**(2):896-904.
35. Nishikawa H, Sakaguchi S: **Regulatory T cells in tumor immunity.** *International journal of cancer* 2010, **127**(4):759-767.
36. Ramello MC, Tosello Boari J, Canale FP, Mena HA, Negrotto S, Gastman B, Gruppi A, Acosta Rodríguez EV, Montes CL: **Tumor-induced senescent T cells promote the secretion of pro-inflammatory cytokines and angiogenic factors by human monocytes/macrophages through a mechanism that involves Tim-3 and CD40L.** *Cell death & disease* 2014, **5**(11):e1507.
37. Buchbinder EI, Desai A: **CTLA-4 and PD-1 Pathways: Similarities, Differences, and Implications of Their Inhibition.** *American journal of clinical oncology* 2016, **39**(1):98-106.
38. Blank C, Mackensen A: **Contribution of the PD-L1/PD-1 pathway to T-cell exhaustion: an update on implications for chronic infections and tumor evasion.** *Cancer immunology, immunotherapy : CII* 2007, **56**(5):739-745.

- 1  
2  
3  
4 39. Gunderson AJ, Yamazaki T, McCarty K, Fox N, Phillips M, Alice A, Blair T, Whiteford  
5  
6 M, O'Brien D, Ahmad R *et al.* **TGF $\beta$  suppresses CD8(+) T cell expression of CXCR3**  
7  
8 **and tumor trafficking.** *Nature communications* 2020, **11**(1):1749.  
9  
10  
11 40. Chen SY, Mamai O, Akhurst RJ: **TGF $\beta$ : Signaling Blockade for Cancer Immunotherapy.**  
12  
13 *Annual review of cancer biology* 2022, **6**(1):123-146.  
14  
15  
16 41. Morisada M, Clavijo PE, Moore E, Sun L, Chamberlin M, Van Waes C, Hodge JW,  
17  
18 Mitchell JB, Friedman J, Allen CT: **PD-1 blockade reverses adaptive immune**  
19  
20 **resistance induced by high-dose hypofractionated but not low-dose daily fractionated**  
21  
22 **radiation.** *Oncoimmunology* 2018, **7**(3):e1395996.  
23  
24  
25 42. Sakuishi K, Apetoh L, Sullivan JM, Blazar BR, Kuchroo VK, Anderson AC: **Targeting**  
26  
27 **Tim-3 and PD-1 pathways to reverse T cell exhaustion and restore anti-tumor immunity.**  
28  
29 *The Journal of experimental medicine* 2010, **207**(10):2187-2194.  
30  
31  
32 43. Son CH, Bae J, Lee HR, Yang K, Park YS: **Enhancement of antitumor immunity by**  
33  
34 **combination of anti-CTLA-4 antibody and radioimmunotherapy through the**  
35  
36 **suppression of Tregs.** *Oncology letters* 2017, **13**(5):3781-3786.  
37  
38  
39 44. Boldt A, Borte S, Fricke S, Kentouche K, Emmrich F, Borte M, Kahlenberg F, Sack U:  
40  
41 **Eight-color immunophenotyping of T-, B-, and NK-cell subpopulations for**  
42  
43 **characterization of chronic immunodeficiencies.** *Cytometry Part B, Clinical cytometry*  
44  
45 2014, **86**(3):191-206.  
46  
47  
48 45. McCaffrey LM, Macara IG: **Epithelial organization, cell polarity and tumorigenesis.**  
49  
50 *Trends in cell biology* 2011, **21**(12):727-735.  
51  
52  
53 46. Wesseling M, Sakkers TR, de Jager SCA, Pasterkamp G, Goumans MJ: **The**  
54  
55  
56  
57  
58  
59  
60

- morphological and molecular mechanisms of epithelial/endothelial-to-mesenchymal transition and its involvement in atherosclerosis. *Vascular pharmacology* 2018, **106**:1-8.
47. Garrido F, Cabrera T, Concha A, Glew S, Ruiz-Cabello F, Stern PL: **Natural history of HLA expression during tumour development.** *Immunology today* 1993, **14**(10):491-499.
48. Classon J, Zamboni M, Engblom C, Alkass K, Mantovani G, Pou C, Nkulikiyimfura D, Brodin P, Druid H, Mold J *et al.* **Prostate cancer disease recurrence after radical prostatectomy is associated with HLA type and local cytomegalovirus immunity.** *Molecular oncology* 2022, **16**(19):3452-3464.
49. Fernandez Vina MA, Hollenbach JA, Lyke KE, Sztejn MB, Maiers M, Klitz W, Cano P, Mack S, Single R, Brautbar C *et al.* **Tracking human migrations by the analysis of the distribution of HLA alleles, lineages and haplotypes in closed and open populations.** *Philosophical transactions of the Royal Society of London Series B, Biological sciences* 2012, **367**(1590):820-829.
50. Manca MA, Simula ER, Cossu D, Solinas T, Madonia M, Cusano R, Sechi LA: **Association of HLA-A\*11:01, -A\*24:02, and -B\*18:01 with Prostate Cancer Risk: A Case-Control Study.** *International journal of molecular sciences* 2023, **24**(20).
51. Mungall AJ, Palmer SA, Sims SK, Edwards CA, Ashurst JL, Wilming L, Jones MC, Horton R, Hunt SE, Scott CE *et al.* **The DNA sequence and analysis of human chromosome 6.** *Nature* 2003, **425**(6960):805-811.
52. Bukur J, Jasinski S, Seliger B: **The role of classical and non-classical HLA class I antigens in human tumors.** *Seminars in cancer biology* 2012, **22**(4):350-358.

1  
2  
3  
4  
5  
6  
7  
8  
9  
10  
11  
12  
13  
14  
15  
16  
17  
18  
19  
20  
21  
22  
23  
24  
25  
26  
27  
28  
29  
30  
31  
32  
33  
34  
35  
36  
37  
38  
39  
40  
41  
42  
43  
44  
45  
46  
47  
48  
49  
50  
51  
52  
53  
54  
55  
56  
57  
58  
59  
60

For Peer Review

**Declarations**

**Ethics approval and consent to participate**

Prior to participation in this study, all patients provided informed consent for the use of their information and specimens for research purposes.

**Consent for publication**

Not applicable.

**Data availability statement**

Availability of data and materials: The datasets used and/or analyzed during the current study are available from the corresponding author on reasonable request.

**Conflict of interest**

The authors declare that the research was conducted in the absence of any commercial or financial relationships that could be construed as a potential conflict of interest.

**Funding**

This work was supported by grants from the Zunyi Science and Technology Department (CK-1350-043).

**Author contributions**

Quan Zhang Study conceptualization and design. Data collection. Study analysis and interpretation of data. Draft and revise manuscript. Prepare tables and figures. Approved submitted version. Bochen Pan (Corresponding author) Data collection. Draft and revise manuscript. Study analysis and interpretation of data. Approved submitted version.

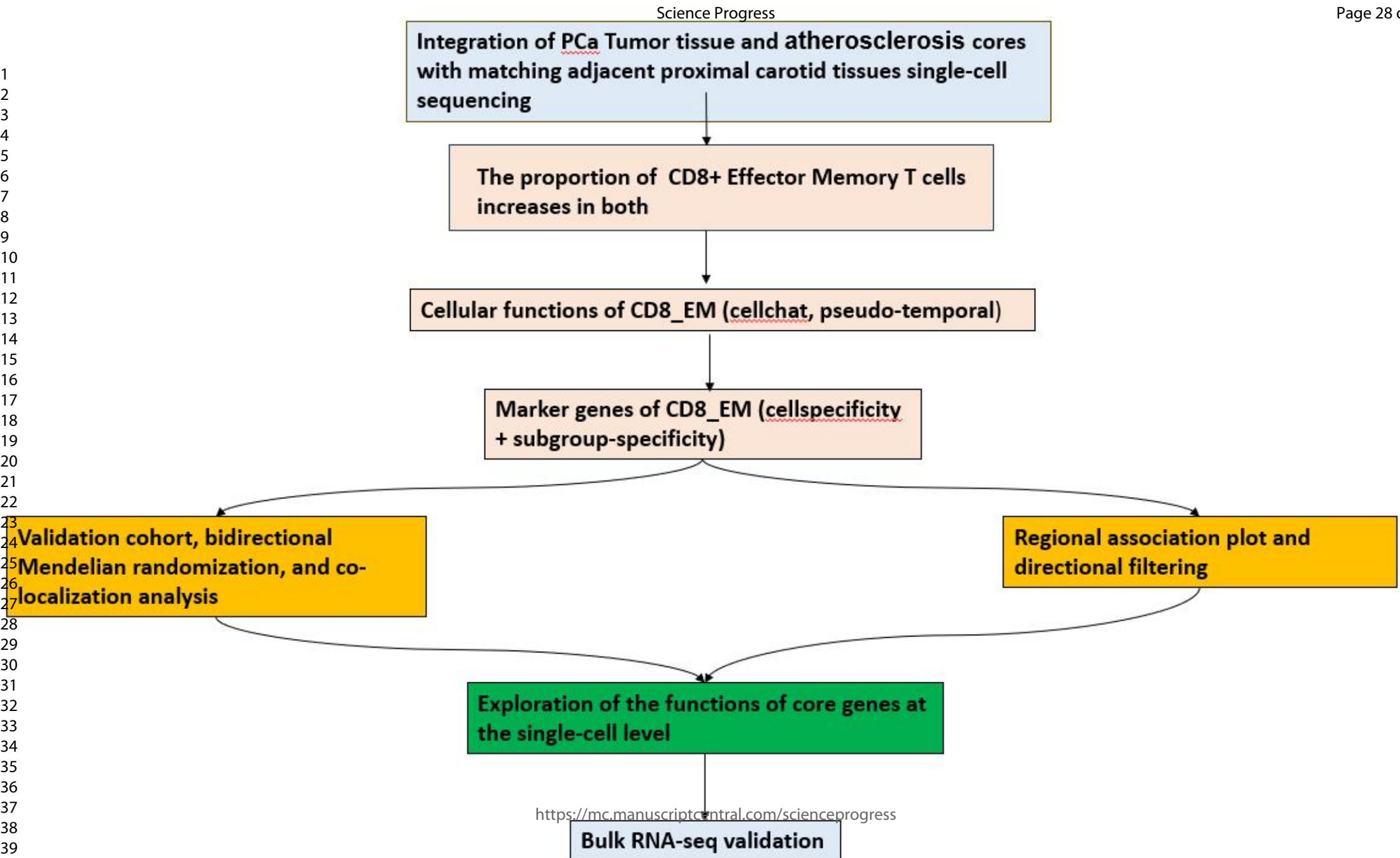
**Publisher’s note**

All claims expressed in this article are solely those of the authors and do not necessarily represent those of their affiliated organizations, or those of the publisher, the editors and the reviewers. Any product that may be evaluated in this article, or claim that may be made by its manufacturer, is not guaranteed or endorsed by the publisher.

**Supplementary material**

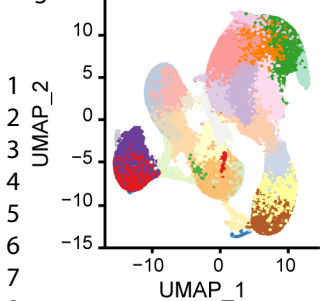
The Supplementary Material for this article can be found online at:

1  
2  
3  
4  
5  
6  
7  
8  
9  
10  
11  
12  
13  
14  
15  
16  
17  
18  
19  
20  
21  
22  
23  
24  
25  
26  
27  
28  
29  
30  
31  
32  
33  
34  
35  
36  
37  
38  
39  
40



A

Page 29 of 44



B

Science Progress

CD34



CD69



EPCAM



C

CD68



TAGLN



PECAM1



LYZ

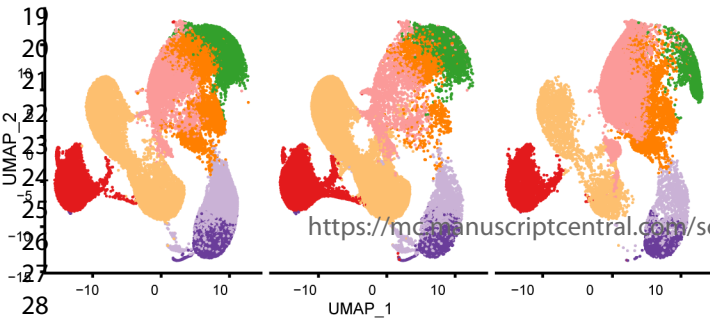


D

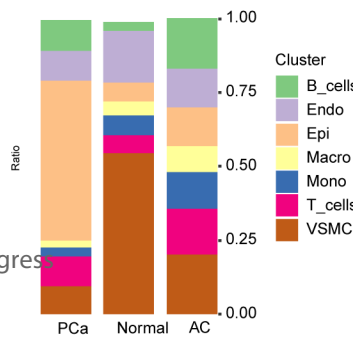
AC

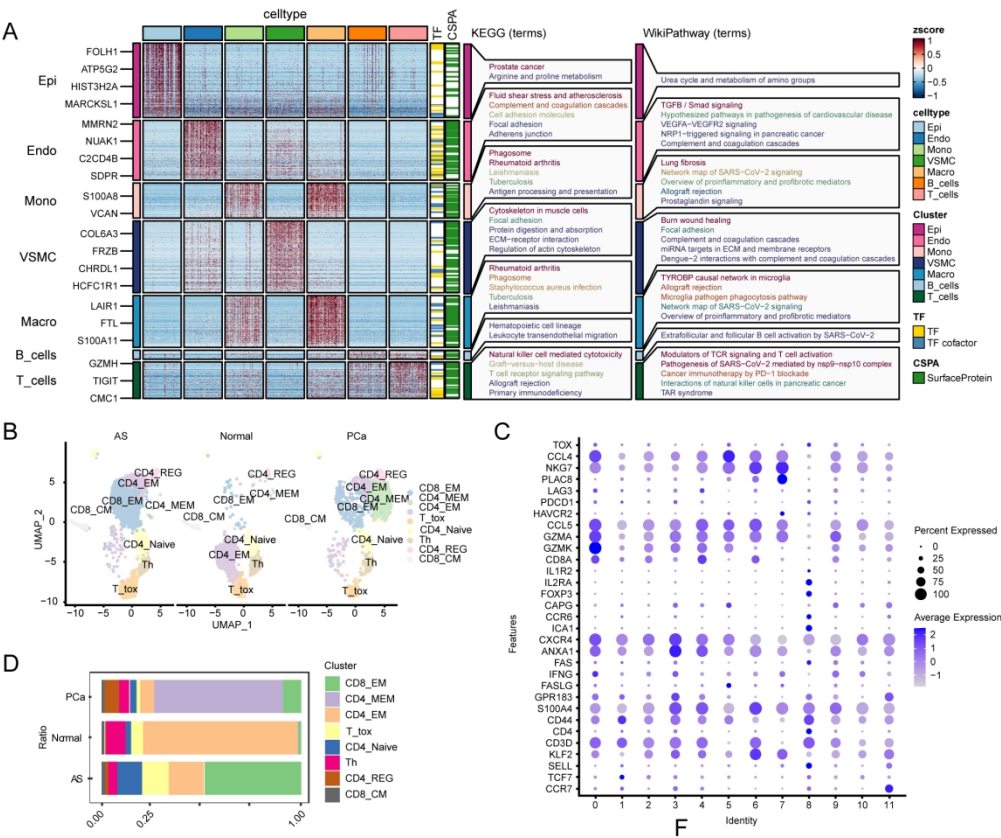
Normal

PCa



E





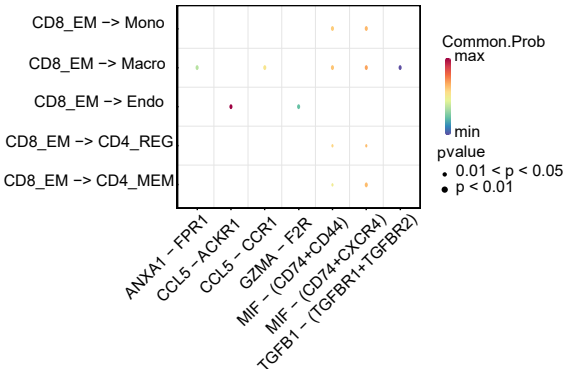
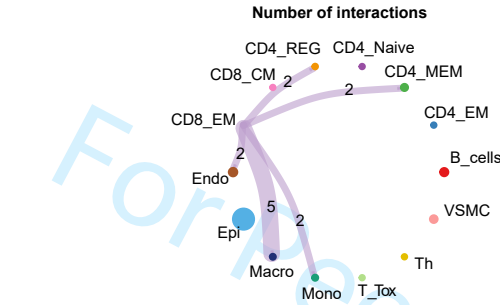
178x149mm (300 x 300 DPI)

1  
2  
3  
4  
5  
6  
7  
8  
9  
10  
11  
12  
13  
14  
15  
16  
17  
18  
19  
20  
21  
22  
23  
24

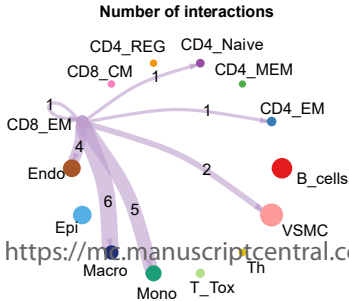
B

Science Progress

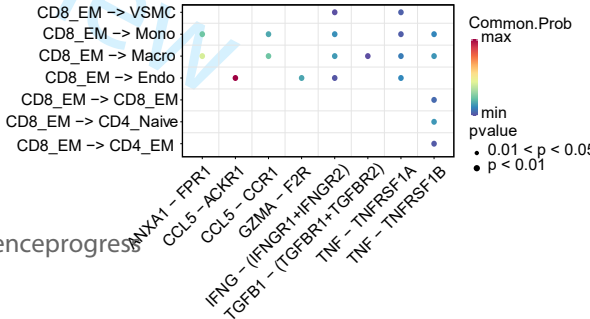
C



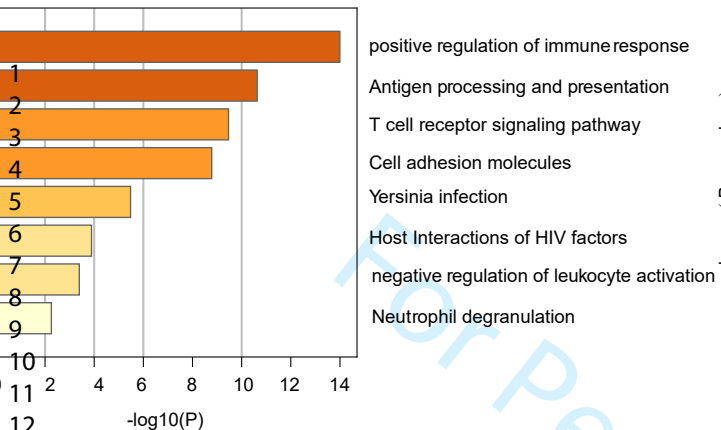
D



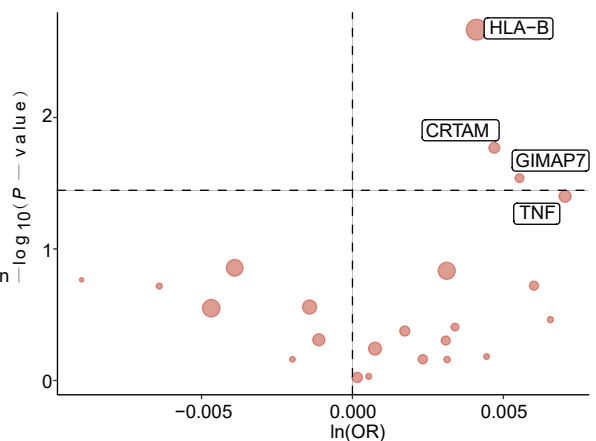
E



A



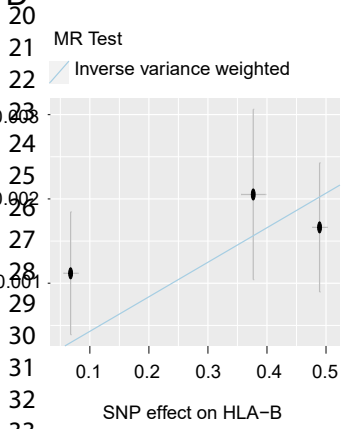
B



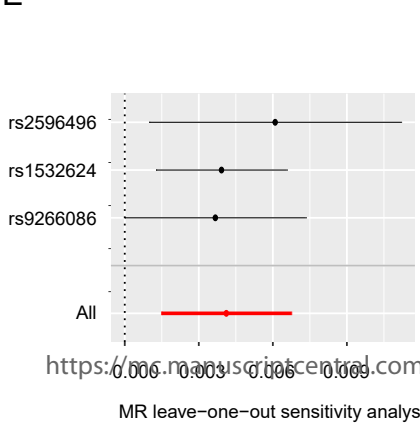
C

exposure	method	n SNP	pval	OR (95% CI)
CRTAM	Inverse variance weighted	3	0.016999070	1.0047 (1.0008 – 1.0086)
GIMAP7	Inverse variance weighted	2	0.028917820	1.0055 (1.0006 – 1.0106)
TNF	Inverse variance weighted	3	0.039735208	1.0071 (1.0003 – 1.0138)
HLA-B	Inverse variance weighted	3	0.002149937	1.0041 (1.0015 – 1.0068)

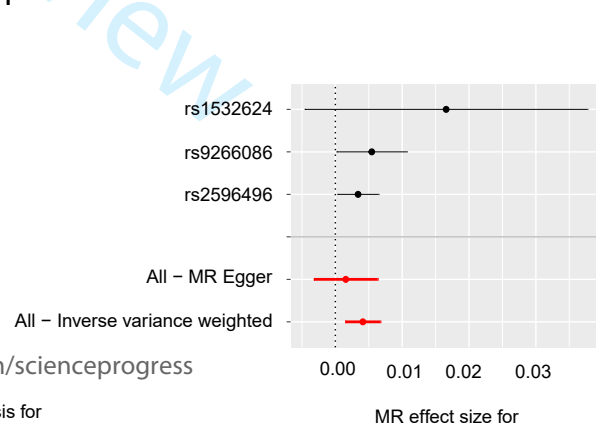
D



E



F

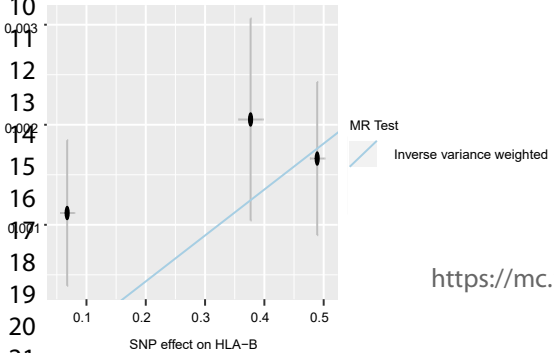


Science Progress

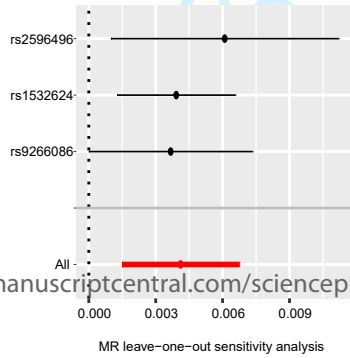
exposure	method	nsnp	pval	OR (95% CI)
HLA-A	Inverse variance weighted	7	4.038900e-02	1.0434 (1.0019 – 1.0867)
TNF	Inverse variance weighted	3	1.326896e-02	1.1606 (1.0316 – 1.3059)
HLA-B	Inverse variance weighted	4	9.177152e-04	1.0901 (1.0359 – 1.1471)

exposure	method	nsnp	pval	outcome	OR (95% CI)
Prostate cancer    id:ieu-b-4809	Inverse variance weighted	18	0.8102630	HLA-B	1.0970 (0.5153 – 2.3354)

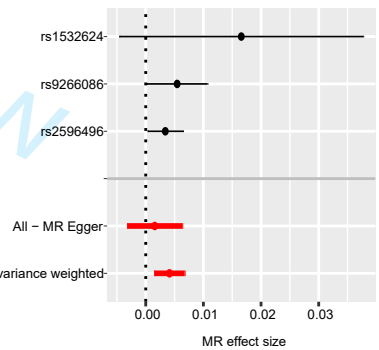
1  
2  
3  
4  
5  
6  
7  
8  
9  
10  
11  
12  
13  
14  
15  
16  
17  
18  
19  
20  
21

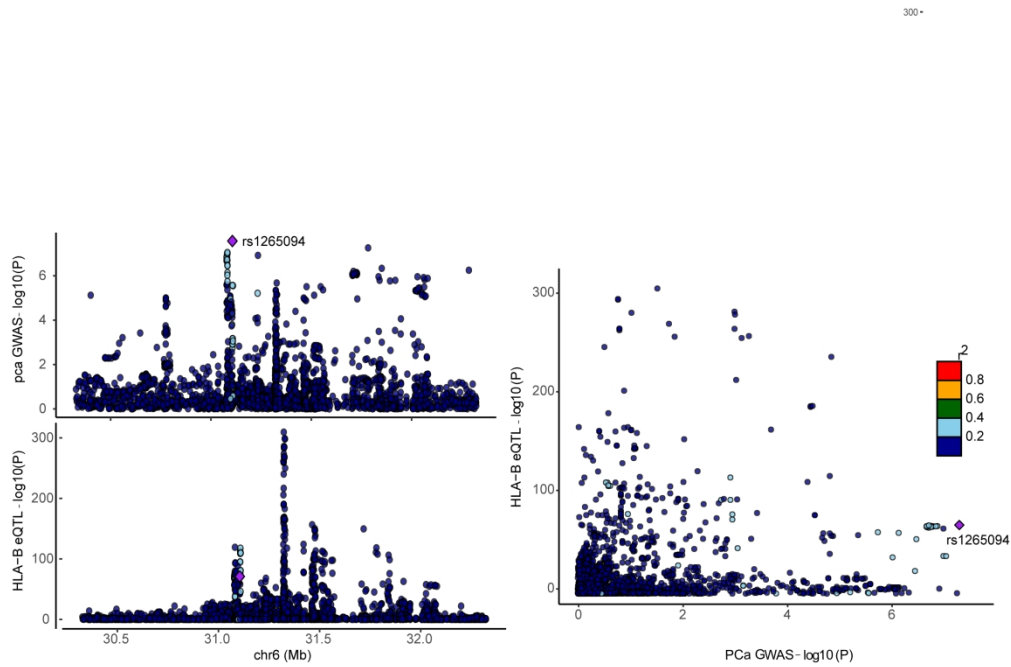


D



E





236x155mm (300 x 300 DPI)

1	
2	Table1: 30 Key Genes
3	GZMK
4	HLA-A
5	HLA-B
6	CCL5
7	GZMA
8	CD8A
9	CD8B
10	IL32
11	CCL4
12	TRBC2
13	PTPRC
14	TNFSF9
15	DUSP2
16	TRAC
17	CCL4L2
18	CST7
19	ITM2C
20	CD2
21	CD3G
22	COTL1
23	CRTAM
24	KIAA1551
25	FYB1
26	RGCC
27	CYT0R
28	APOBEC3G
29	TERF2IP
30	GIMAP7
31	TNF
32	IFNG
33	
34	
35	
36	
37	
38	
39	
40	
41	
42	
43	
44	
45	
46	
47	
48	
49	
50	
51	
52	
53	
54	
55	
56	
57	
58	
59	
60	

For Peer Review

Table2: Results of the Heterogeneity Analysis of Key Genes

id.exposure	id.outcome	outcome	exposure
eqtl-a-ENSG00000008517	ieu-b-4809	Prostate	IL32
eqtl-a-ENSG00000008517	ieu-b-4809	Prostate	IL32
eqtl-a-ENSG00000077984	ieu-b-4809	Prostate	CST7
eqtl-a-ENSG00000077984	ieu-b-4809	Prostate	CST7
eqtl-a-ENSG00000081237	ieu-b-4809	Prostate	PTPRC
eqtl-a-ENSG00000102760	ieu-b-4809	Prostate	RGCC
eqtl-a-ENSG00000102760	ieu-b-4809	Prostate	RGCC
eqtl-a-ENSG00000103187	ieu-b-4809	Prostate	COTL1
eqtl-a-ENSG00000103187	ieu-b-4809	Prostate	COTL1
eqtl-a-ENSG00000109943	ieu-b-4809	Prostate	CRTAM
eqtl-a-ENSG00000109943	ieu-b-4809	Prostate	CRTAM
eqtl-a-ENSG00000111537	ieu-b-4809	Prostate	IFNG
eqtl-a-ENSG00000113088	ieu-b-4809	Prostate	GZMK
eqtl-a-ENSG00000113088	ieu-b-4809	Prostate	GZMK
eqtl-a-ENSG00000116824	ieu-b-4809	Prostate	CD2
eqtl-a-ENSG00000116824	ieu-b-4809	Prostate	CD2
eqtl-a-ENSG00000135916	ieu-b-4809	Prostate	ITM2C
eqtl-a-ENSG00000135916	ieu-b-4809	Prostate	ITM2C
eqtl-a-ENSG00000145649	ieu-b-4809	Prostate	GZMA
eqtl-a-ENSG00000145649	ieu-b-4809	Prostate	GZMA
eqtl-a-ENSG00000153563	ieu-b-4809	Prostate	CD8A
eqtl-a-ENSG00000153563	ieu-b-4809	Prostate	CD8A
eqtl-a-ENSG00000172116	ieu-b-4809	Prostate	CD8B
eqtl-a-ENSG00000179144	ieu-b-4809	Prostate	GIMAP7
eqtl-a-ENSG00000206503	ieu-b-4809	Prostate	HLA-A
eqtl-a-ENSG00000206503	ieu-b-4809	Prostate	HLA-A
eqtl-a-ENSG00000232810	ieu-b-4809	Prostate	TNF
eqtl-a-ENSG00000232810	ieu-b-4809	Prostate	TNF
eqtl-a-ENSG00000234745	ieu-b-4809	Prostate	HLA-B
eqtl-a-ENSG00000234745	ieu-b-4809	Prostate	HLA-B
eqtl-a-ENSG00000239713	ieu-b-4809	Prostate	APOBEC3G
eqtl-a-ENSG00000239713	ieu-b-4809	Prostate	APOBEC3G

1  
2  
3  
4  
5  
6  
7  
8  
9  
10  
11  
12  
13  
14  
15  
16  
17  
18  
19  
20  
21  
22  
23  
24  
25  
26  
27  
28  
29  
30  
31  
32  
33  
34  
35  
36  
37  
38  
39  
40  
41  
42  
43  
44  
45  
46  
47  
48  
49  
50  
51  
52  
53  
54  
55  
56  
57  
58  
59  
60

method	Q	Q_df	Q_pval
MR Egger	16.76066	3	0.000792
Inverse variance weighted	16.88585	4	0.002034
MR Egger	3.411617	3	0.332407
Inverse variance weighted	3.872456	4	0.423542
Inverse variance weighted	2.946007	1	0.08609
MR Egger	0.84102	2	0.656712
Inverse variance weighted	1.097335	3	0.777718
MR Egger	0.045382	1	0.831303
Inverse variance weighted	3.395116	2	0.18313
MR Egger	1.591641	1	0.207092
Inverse variance weighted	2.30441	2	0.315939
Inverse variance weighted	3.371787	1	0.066322
MR Egger	11.38934	7	0.122515
Inverse variance weighted	12.35774	8	0.135942
MR Egger	0.971634	1	0.324273
Inverse variance weighted	0.986044	2	0.610778
MR Egger	1.701652	5	0.888692
Inverse variance weighted	2.859373	6	0.826279
MR Egger	3.170805	2	0.204865
Inverse variance weighted	5.064599	3	0.167128
MR Egger	25.23639	4	4.51E-05
Inverse variance weighted	31.57361	5	7.22E-06
Inverse variance weighted	0.059041	1	0.808018
Inverse variance weighted	0.774792	1	0.378739
MR Egger	21.6258	5	0.000617
Inverse variance weighted	22.10063	6	0.001161
MR Egger	3.811911	1	0.050889
Inverse variance weighted	3.906753	2	0.141795
MR Egger	0.208695	1	0.647792
Inverse variance weighted	1.789892	2	0.40863
MR Egger	2.623061	4	0.622743
Inverse variance weighted	2.623879	5	0.757734

Table3: Results of the Horizontal Pleiotropy Analysis of Key Genes

id.exposure	id.outcome	outcome	exposure	egger_intse	pval
eqtl-a-ENSG00000008517	ieu-b-4809	Prostate	IL32	-0.00019 0.001285	0.890502
eqtl-a-ENSG000000077984	ieu-b-4809	Prostate	CST7	-0.00044 0.000695	0.569645
eqtl-a-ENSG000000081237	ieu-b-4809	Prostate	PTPRC	NA NA	NA
eqtl-a-ENSG000000102760	ieu-b-4809	Prostate	RGCC	-0.00038 0.000754	0.662956
eqtl-a-ENSG000000103187	ieu-b-4809	Prostate	COTL1	0.002066 0.001129	0.318348
eqtl-a-ENSG000000109943	ieu-b-4809	Prostate	CRTAM	0.000975 0.001458	0.624553
eqtl-a-ENSG000000111537	ieu-b-4809	Prostate	IFNG	NA NA	NA
eqtl-a-ENSG000000113088	ieu-b-4809	Prostate	GZMK	0.000634 0.000821	0.46566
eqtl-a-ENSG000000116824	ieu-b-4809	Prostate	CD2	-0.00019 0.001568	0.923944
eqtl-a-ENSG000000135916	ieu-b-4809	Prostate	ITM2C	-0.00059 0.00055	0.331094
eqtl-a-ENSG000000145649	ieu-b-4809	Prostate	GZMA	0.00103 0.000942	0.388504
eqtl-a-ENSG000000153563	ieu-b-4809	Prostate	CD8A	0.001493 0.00149	0.372946
eqtl-a-ENSG000000172116	ieu-b-4809	Prostate	CD8B	NA NA	NA
eqtl-a-ENSG000000179144	ieu-b-4809	Prostate	GIMAP7	NA NA	NA
eqtl-a-ENSG000000206503	ieu-b-4809	Prostate	HLA-A	0.00038 0.001147	0.753827
eqtl-a-ENSG000000232810	ieu-b-4809	Prostate	TNF	0.000495 0.003139	0.900403
eqtl-a-ENSG000000234745	ieu-b-4809	Prostate	HLA-B	0.001068 0.000849	0.427708
eqtl-a-ENSG000000239713	ieu-b-4809	Prostate	APOBEC3G	1.64E-05 0.000574	0.978552

1  
2  
3  
4  
5  
6  
7  
8  
9  
10  
11  
12  
13  
14  
15  
16  
17  
18  
19  
20  
21  
22  
23  
24  
25  
26  
27  
28  
29  
30  
31  
32  
33  
34  
35  
36  
37  
38  
39  
40  
41  
42  
43  
44  
45  
46  
47  
48  
49  
50  
51  
52  
53  
54  
55  
56  
57  
58  
59  
60

For Peer Review

Table4: Results of the Reverse Mendelian Randomization Analysis of the HLA-B Gene

id. exposure	outcome	exposure
ebi-a-GCST90018	eqtl-a-ENSG000000:Prostate cancer	id:ebi-a-GCST90018905

For Peer Review

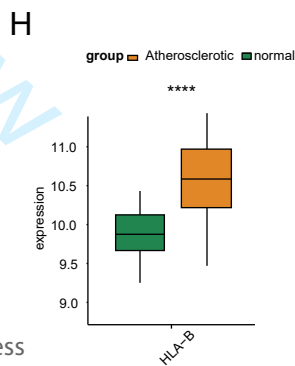
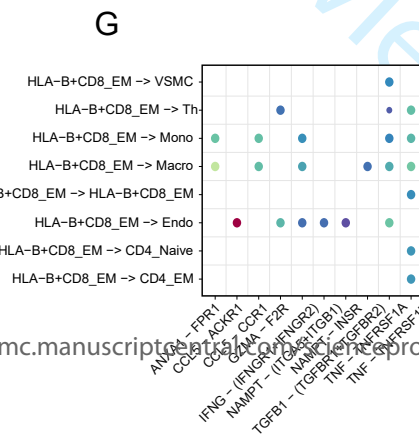
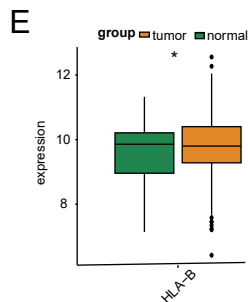
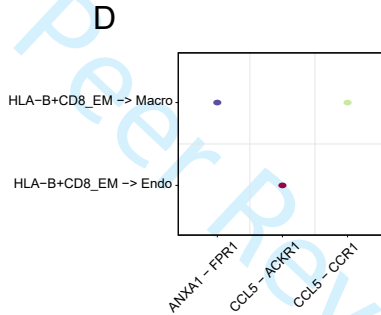
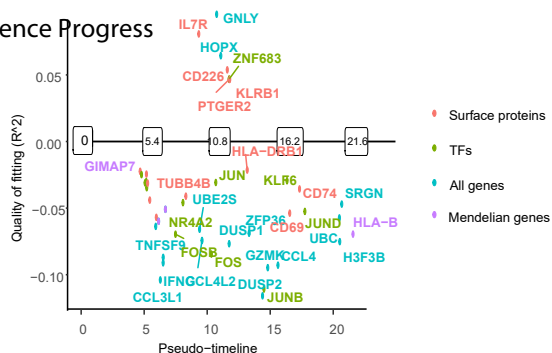
1  
2  
3  
4  
5  
6  
7  
8  
9  
10  
11  
12  
13  
14  
15  
16  
17  
18  
19  
20  
21  
22  
23  
24  
25  
26  
27  
28  
29  
30  
31  
32  
33  
34  
35  
36  
37  
38  
39  
40  
41  
42  
43  
44  
45  
46  
47  
48  
49  
50  
51  
52  
53  
54  
55  
56  
57  
58  
59  
60

method	nsnp	b	se	pval	lo_ci	up_ci	or
MR Egger	16	-0.0211	0.055256	0.708302	-0.1294	0.087202	0.979121
Weighted median	16	0.011798	0.024414	0.628904	-0.03605	0.059649	1.011868
Inverse variance	16	0.016599	0.025715	0.518604	-0.0338	0.066999	1.016737
Simple mode	16	-0.0021	0.036123	0.954311	-0.07291	0.068697	0.997898
Weighted mode	16	0.006355	0.026162	0.811357	-0.04492	0.057632	1.006375

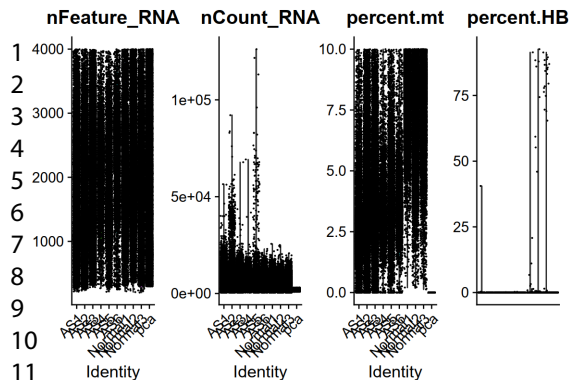
For Peer Review

<u>or_lci95 or_uci95</u>	
0.878621	1.091117
0.96459	1.061464
0.966763	1.069295
0.929688	1.071112
0.956073	1.059325

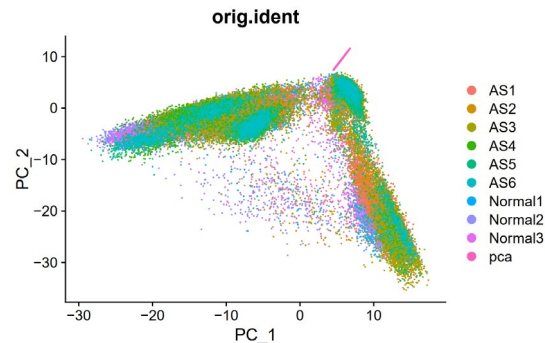
For Peer Review



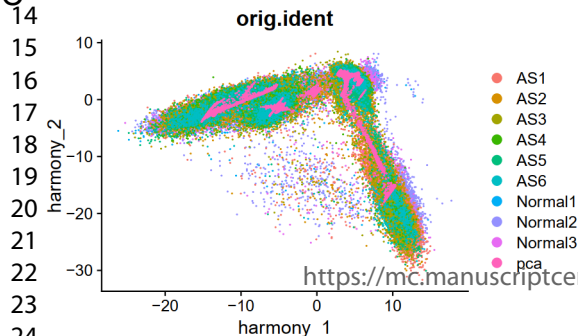
A



B



C



D

